Rheology of Nematic Side-Chain Liquid-Crystalline Polymer: Comparison with Main-Chain Liquid-Crystalline Polymer

Kyung Min Lee and Chang Dae Han*

Department of Polymer Engineering, The University of Akron, Akron, Ohio 44325

Received December 26, 2001

ABSTRACT: A nematic side-chain liquid-crystalline polymer (SCLCP) was synthesized by grafting a liquid-crystalline monomer, 6-[(4-cyano-4′-biphenyl)oxy]hexanoic acid (5CN-COOH), onto a nearly monodisperse hydroxylated polyisoprene. The linear dynamic viscoelasticity, steady shear flow, transient and intermittent shear flows, and stress relaxation of the SCLCP in the nematic state were investigated. For comparison, the rheological behavior of a main-chain liquid-crystalline polymer (MCLCP) was also investigated. Similarities and dissimilarities in the rheological behavior between the SCLCP and MCLCP are presented. Some of the important similarities observed are as follows. Upon start-up of shear flow, both SCLCP and MCLCP exhibited a very large overshoot peak of first normal stress difference (N_1^+) and shear stress (σ^+). The values of first normal stress difference in steady shear flow were *positive* in both SCLCP and MCLCP over the entire range of shear rates tested. Some of the important dissimilarities observed are as follows. The steady-state shear viscosity (η) of the SCLCP exhibited a Newtonian behavior at shear rates as low as 0.01 s^{-1} followed by a shear-thinning behavior at higher shear rates, similar to ordinary flexible polymers, whereas the η of the MCLCP exhibited a shear-thinning behavior at low shear rates followed by a Newtonian region at intermediate shear rates and then another shear-thinning behavior at higher shear rates. During intermittent shear flow that was initiated after a rest for 1 h after cessation of steady shear flow, both N_1^+ and σ^+ of the SCLCP exhibited a large overshoot peak, the magnitude of which was *almost the same* as that upon start-up of shear flow, whereas the magnitude of the overshoot peak in both N_1^+ and σ^+ of the MCLCP during intermittent shear flow was much smaller than that upon start-up of shear flow. Upon cessation of steady shear flow, the dynamic storage and loss moduli (G' and G''), which were monitored at a very low angular frequency, of the SCLCP increased initially very rapidly and then leveled off within ca. 40 min, whereas the G' and G'' of the MCLCP did not level off in the same period. Upon cessation of steady shear flow, both shear stress and first normal stress difference of the SCLCP relaxed much faster than those of the MCLCP did.

1. Introduction

Today it is well recognized that the rheological behavior of liquid-crystalline polymers (LCPs) is much more complex than that of ordinary flexible polymers. The complexity in the rheological behavior of LCPs arises from the fact that the flow imposed greatly influences the structure and orientation of the mesophase in the fluid. It is then clear that the flow and orientation and the flow and the structure of the mesophase are inseparable in the understanding of the rheological behavior of LCPs. Therefore, a combination of rheometry and birefringence[1−10] or X-ray scattering[7,11−16] has been employed to investigate flow−orientation relationships in LCPs, and a combination of rheometry and optical microscopy[8,9,12,13,17−20] or small-angle light scattering[8,9,21,22] has been employed to investigate flow−morphology relationships in LCPs.

The rheological behavior of lyotropic LCP can be different and perhaps more complicated than that of thermotropic LCP, because the rheological behavior of lyotropic LCP may depend on the choice of solvents that were used to prepare the solutions. In the past, a number of investigators reported on the rheology of solutions of poly(*p*-benzamide) (PBA) dissolved in DMAc−LiCl,[23−25] solutions of poly(benzylglutamate) (PBG) or poly(γ-benzyl-L-glutamate) (PBLG) in *m*-cresol,[5,26−33] and aqueous solutions of hydroxypropylcellulose.[34−36] One well-known example that distinguishes the rheological behavior of lyotropic LCP from that of thermotropic LCP is that *negative* first normal stress difference (N_1) in steady shear flow has been observed only for lyotropic LCPs. Specifically, several research groups[27,37−41] have reported experimental observations of *negative* values of N_1 in lyotropic LCPs, while only *positive* values of N_1 have been reported in thermotropic LCPs.[16,42−49] It is fair to state that within the past decade there have been more extensive rheological investigations on thermotropic LCPs than on lyotropic LCPs.

There are two types of thermotropic LCP: main-chain LCP (MCLCP) and side-chain LCP (SCLCP). While the investigation of the rheology of MCLCP started in the 1970s, the active investigations of the rheology of SCLCP have been reported within the past decade.[50−62] Kornfield and co-workers[53−55] and Berghausen et al.[57] reported on the effect of shear on the flow alignment of SCLCP, and Quijada-Garrido et al.[59,60] reported on the transient shear flow and flow reversal of SCLCP. However, little has been reported on a vis-à-vis comparison of the rheological behavior between SCLCP and MCLCP.

Very recently, we synthesized a *nearly monodisperse* nematic-forming SCLCP. This is significant in that almost all the SCLCPs reported in the literature have been synthesized by condensation polymerization, invariably giving rise to polydisperse SCLCPs. Using the SCLCP, we investigated linear dynamic viscoelasticity, steady shear-flow properties, transient and intermittent shear flows, stress relaxation, and time evolution of dynamic storage and loss moduli upon cessation of shear flow at different temperatures in the nematic state. We then compared vis-à-vis the rheological behavior of the

10.1021/ma012240k CCC: $22.00
Published on Web 06/26/2002

Scheme 1

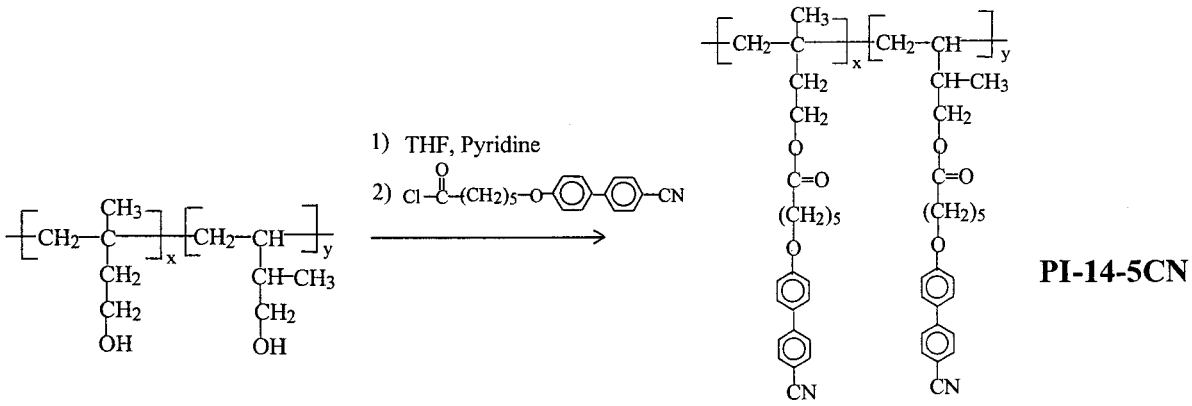

SCLCP with that of an MCLCP. In this paper we present the highlights of our findings.

2. Experimental Section

Materials and Characterization. We first synthesized, via anionic polymerization, a polyisoprene (PI) having predominantly 1,2- and 3,4-addition, and a number-average molecular weight (M_n) of 1.43×10^4 g/mol as determined by membrane osmometry (Jupiter Instrument) and a polydispersity index (M_w/M_n) of 1.05 as determined by gel permeation chromatography (GPC, Waters). Hereafter, the PI synthesized will be referred to as PI-14. Subsequently, PI-14 was hydroxylated, via hydroboration/oxidation reactions, to obtain a nearly monodisperse hydroxylated PI (PI-14-OH). The details of the hydroboration/oxidation procedures are described in our recent paper.[63]

A liquid crystalline monomer, 6-[(4-cyano-4′-biphenyl)oxy]-hexanoic acid, with the chemical structure

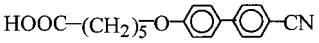

was synthesized. Hereafter this structure will be referred to as 5CN-COOH. Subsequently, 5CN-COOH was chlorinated to obtain 5CN-COCl. The details of the synthesis of 5CN-COOH and chlorination procedures are described in our previous paper.[64] The grafting of 5CN-COCl onto the PI-14-OH was accomplished by the reaction route shown in Scheme 1. Briefly stated, a predetermined amount of PI-14-OH (1 mol of OH), which was just dried in a vacuum oven at 40 °C, was dissolved in a 10 mL mixture of anhydrous tetrahydrofuran (THF) and pyridine (1:1 v/v) in a three-necked flask with stirrer at room temperature under argon gas. After stirring for 1 h, 1.2 mol of 5CN-COCl solution in anhydrous THF was added dropwise into the reaction flask for 30 min at 0 °C; the reaction temperature was increased gradually to room temperature and maintained there for 24 h. The reaction mixture was poured into ethanol/water (1:1 v/v), and the crude product was precipitated, which was then filtered and washed several times with ethanol/water (1:1 v/v). The polymer was extracted with methanol using a Soxhlet extractor for 5 days. Subsequently, the final product, PI-14-5CN, was dried in a vacuum oven at 30 °C for 2 days and at 60 °C for 1 day. The chemical structure of PI-14-5CN was confirmed using ^{1}H NMR spectroscopy and Fourier transform infrared (FTIR) spectroscopy.

An accurate determination of the molecular weight of PI-14-5CN from the GPC trace was not possible since information on the hydrodynamic volume of PI-14-5CN was unavailable. Therefore, we calculated the molecular weight of PI-14-5CN to be 7.19×10^4 g/mol using information on the degree of hydroxylation. The polydispersity of PI-14-5CN determined from GPC is found to be 1.08.

Although the primary purpose of this study was to investigate the rheological behavior of the SCLCP, PI-14-5CN, we also decided to compare the rheological behavior of PI-14-5CN vis-à-vis with that of an MCLCP. Thus, we also investigated the rheological behavior of an MCLCP, poly[(phenylsulfonyl)-*p*-phenylene nonanemethylene bis(4-oxybenzoate)] (PSHQ9), with the chemical structure

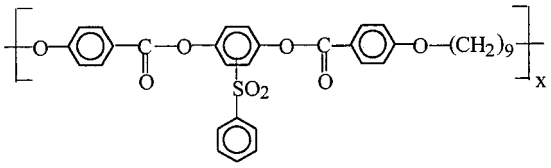

which was synthesized earlier by Chang and Han.[65] The details of the synthesis procedures for PSHQ9 are described elsewhere.[66,67] According to Chang and Han,[65] PSHQ9 has an intrinsic viscosity of 0.823 dL/g at 23 °C, a glass transition temperature (T_g) of 84 °C, and a nematic-to-isotropic (N−I) transition temperature (T_{NI}) of 162 °C. It should be mentioned that PSHQ9 has only nematic phase at temperatures between T_g and T_{NI}, and it is a glassy polymer.

Differential Scanning Calorimetry (DSC). Thermal transition temperatures of all specimens of 5CN-COOH and PI-14-5CN were determined using differential scanning calorimetry (Perkin-Elmer 7 series), under a nitrogen atmosphere, at a heating rate of 20 °C/min. The DSC traces for 5CN-COOH are given in Figure 1a, showing that 5CN-COOH has a clearing temperature (T_{cl}) of 170 °C on heating and 156 °C on cooling. The DSC traces of PI-14-5CN are given in Figure 1b, showing that PI-14-5CN undergoes glass transition at 45 °C and N−I transition at 102 °C. Notice in Figure 1b that PI-14-5CN is a glassy polymer. Comparison of parts a and b of Figure 1 reveals that the T_{cl} of 5CN-COOH, after being grafted onto the PI-14-OH, is decreased considerably.

In our previous paper,[64] we presented experimental evidence via FTIR that the rather high T_{cl} of 5CN-COOH is attributable to the presence of hydrogen bonding.

Polarizing Optical Microscopy (POM). A hot-stage (TH-600 type, Linkham Scientific) microscope (Nikon, model Optiphoto polXTP-11) with a camera, a programmable temperature controller, and photomicrographic attachment was used to take pictures, under cross-polarized light.

Specimens were cast from toluene (1 wt % solution) on a slide glass to obtain a film sample of about 2−3 μm in thickness, which was then dried first in a fume hood and then in a vacuum oven. The inset in Figure 1a gives a POM image of 5CN-COOH at 142 °C during the cooling cycle showing two and four brushes, suggesting that 5CN-COOH has a nematic phase. The inset in Figure 1b gives a POM image of PI-14-5CN at 75 °C showing the presence of a nematic phase.

Rheological Measurements. Specimens for rheological measurements were prepared by first dissolving each polymer in THF in the presence of 0.1 wt % antioxidant (Irganox 1010, Ciba-Geigy Group) and then slowly evaporating the solvent

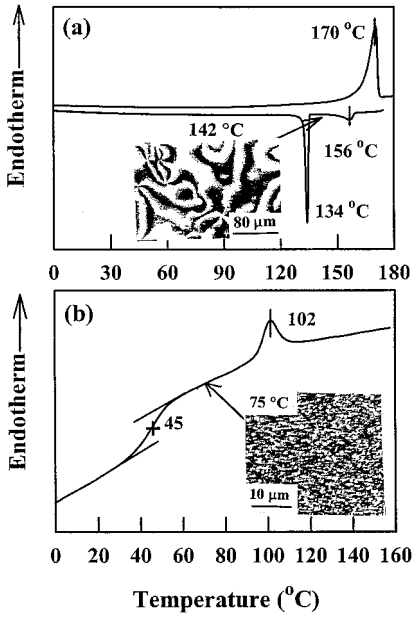

Figure 1. (a) DSC traces of 5CN-COOH in the second heating and cooling cycles at a rate of 20 °C/min. A POM image of 5CN-COOH at 142 °C is given in the inset. (b) DSC trace of PI-14-5CN in the second heating cycle at a rate of 20 °C/min. A POM image of PI-14-5CN at 75 °C is given in the inset.

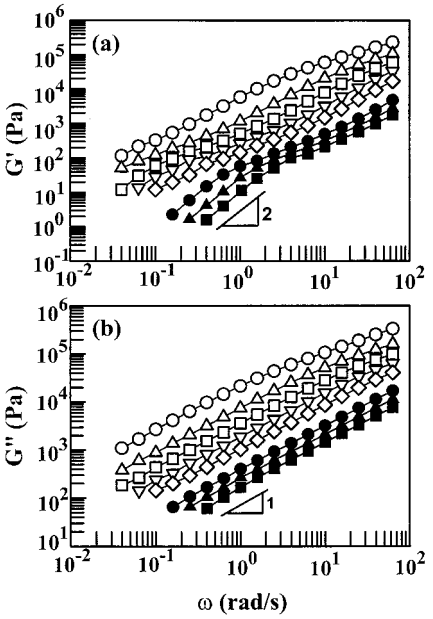

Figure 2. (a) Plots of log G' vs log ω and (b) plots of log G'' vs log ω for PI-14-5CN (SCLCP) at various temperatures: (○) 75, (△) 80, (□) 85, (▽) 90, (◇) 95, (●) 105, (▲) 110, and (■) 115 °C.

at room temperature for 1 week. The cast films (1 mm thick) were further dried in a vacuum oven at room temperature for at least 3 weeks and, prior to measurements, at 60 °C for 48 h to remove any residual solvent and moisture. An Advanced Rheometric Expansion System (ARES, Rheometric Scientific) with a cone-and-plate (8 mm diameter plate, 0.1 rad cone angle) fixture, the gap opening at the apex of the cone and plate being set to 50 μm, was used to investigate steady-state shear flow, transient shear flow, intermittent shear flow, and stress relaxation upon cessation of shear flow. For the transient and intermittent shear flows and stress relaxation experiments, both shear stress growth (or decay) and first normal stress difference growth (or decay) were recorded as functions of time at a shear rate ($\dot{\gamma}$) of 0.1, 0.5, or 1.0 s^{-1} and at 70 °C in the nematic phase of PI-14-5CN and at 130 °C in the nematic phase of PSHQ9. Intermittent shear flow experiment was conducted after waiting for 1 h upon cessation of steady-state shear flow. We also conducted oscillatory shear flow experiments with a parallel-plate (8 mm diameter plate) fixture, the gap opening being set to 0.5 mm, to measure the dynamic storage and loss moduli (G' and G'') of PI-14-5CN and PSHQ9, respectively, as functions of angular frequencies (ω) in the range from 0.04 to 100 rad/s. Further, upon cessation of shear flow, values of G' and G'' were monitored at $\omega = 1$ rad/s for as long as 120 min. All experiments were conducted under a nitrogen atmosphere to minimize oxidative degradation of the specimens. Temperature control was satisfactory to within ±1 °C.

3. Results and Discussion

Linear Viscoelasticity. Figure 2 gives plots of log G' vs log ω, and log G'' vs log ω, for PI-14-5CN, which is an SCLCP, at various temperatures. It is seen that the slope of log G' vs log ω plots over the entire range of ω tested remains less than 2 at temperatures below ca. 105 °C, and then the slope in the terminal region becomes 2 when the temperature is increased to 105 °C and higher. This temperature is close to the T_{NI} (102 °C) of PI-14-5CN determined from DSC (see Figure 1b). The frequency dependence of G' shown in Figure 2a makes sense, because at temperatures below T_{NI} PI-14-5CN is in an anisotropic state forming the nematic phase and at temperatures above T_{NI} PI-14-5CN becomes a homogeneous liquid, and thus it is expected to exhibit a liquidlike behavior in the terminal region. On the other hand, log G'' vs log ω plots given in Figure 2b exhibit a liquidlike behavior over the entire range of temperatures tested, indicating that the dynamic loss modulus G'' of PI-14-5CN is not as sensitive as the dynamic storage modulus G' to a variation in the morphological state from the nematic phase to the isotropic phase as the temperature is increased. Earlier, Colby et al.[58] synthesized nematic SCLCPs, in which *trans*-azobenzene mesogens with six methylene groups as flexible spacers were grafted onto the acrylate or methacrylate backbones, and then investigated dynamic linear viscoelastic properties of the SCLCPs in both the nematic and isotropic states. Applying time−temperature superposition to the plots of log G' vs log ω and log G'' vs log ω, Colby et al. concluded that the dynamic linear viscoelastic properties of the SCLCPs were qualitatively similar to those of ordinary flexible linear polymers. The frequency dependence of G'' for PI-14-5CN given in Figure 2b is consistent with the observation made earlier by Colby et al., but the frequency dependence of G' for PI-14-5CN given in Figure 2a is certainly at variance with the observation made by Colby et al. with their SCLCPs. The frequency dependence of G' given in Figure 2a has never been observed in ordinary flexible linear polymers.

For comparison, let us look at the frequency dependence of G' and G'' for PSHQ9, which is an MCLCP, at various temperatures given in Figure 3. It is seen from Figure 3a that at very low values of ω (say at $\omega < 0.1$ rad/s) G' first decreases as temperature is increased from 130 to 150 °C and then increases as the temperature is increased to 160 °C followed by a decrease as the temperature is increased further to 170 °C and higher. It should be remembered that the T_{NI} of PSHQ9 is ca. 162 °C. Thus, the temperature dependence of G' for PSHQ9 is quite different from that for PI-14-5CN (compare Figure 3a with Figure 2a). The temperature dependence of G'' for PSHQ9, given in Figure 3b, appears to be more complicated than that of G' in that

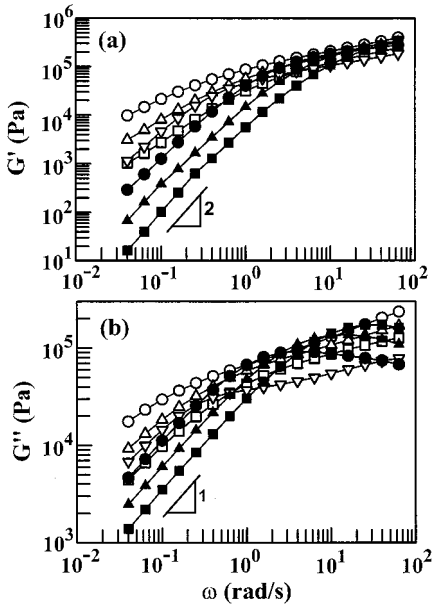

Figure 3. (a) Plots of log G' vs log ω and (b) plots of log G'' vs log ω for PSHQ9 (MCLCP) at various temperatures: (○) 130, (△) 140, (□) 150, (▽) 160, (●) 170, (▲) 180, and (■) 190 °C.

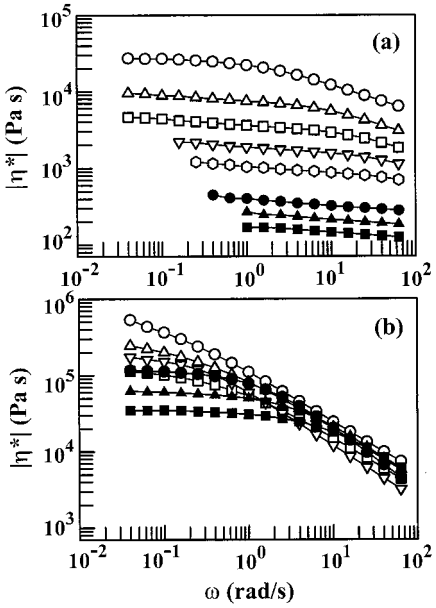

Figure 4. (a) Plots of log $|\eta^*|$ vs log ω for PI-14-5CN (SCLCP) at various temperatures: (○) 75, (△) 80, (□) 85, (▽) 90, (◊) 95, (●) 105, (▲) 110, and (■) 115 °C. (b) Plots of log $|\eta^*|$ vs log ω for PSHQ9 (MCLCP) at various temperatures: (○) 130, (△) 140, (□) 150, (▽) 160, (●) 170, (▲) 180, and (■) 190 °C.

at very low values of ω (say at $\omega < 0.1$ rad/s) the values of G'' at 170 °C, which is above the T_{NI} (162 °C) of PSHQ9, are larger than those at 150 °C. This observation is quite different from that made in Figure 2b for PI-14-5CN. Thus, we conclude that the temperature and frequency dependencies of G' and G'' for PI-14-5CN, which is an SCLCP, are quite different from those for PSHQ9, which is an MCLCP.

Figure 4 gives log $|\eta^*|$ vs log ω plots for (a) PI-14-5CN and (b) PSHQ9 at various temperatures, where $|\eta^*|$ is the complex viscosity defined by $|\eta^*| = [(G'/\omega)^2 + (G''/\omega)^2]^{1/2}$. The following observations are worth noting. The frequency and temperature dependencies of $|\eta^*|$ for PI-14-5CN, given in Figure 4a, look very similar to those often observed for ordinary flexible linear polymers. On the other hand, the frequency and temperature dependencies of $|\eta^*|$ for PSHQ9 are quite complicated as can be seen in Figure 4b. Specifically, (i) the $|\eta^*|$ of PSHQ9 at 130 °C exhibits a shear-thinning behavior over the entire range of angular frequencies tested, (ii) at low angular frequencies (say at $\omega < 0.1$ rad/s) values of $|\eta^*|$ of PSHQ9 at 160 °C are higher than those at 150 °C, and values of $|\eta^*|$ at 170 °C in the isotropic state are very close to or higher than those at 150 °C in the nematic state, and (iii) at higher angular frequencies (say $\omega > 10$ rad/s) the $|\eta^*|$ at 170−190 °C in the isotropic state are higher than those at 150−160 °C in the nematic state. Thus, we conclude that the temperature and frequency dependencies of $|\eta^*|$ for PSHQ9 are different from those for PI-14-5CN.

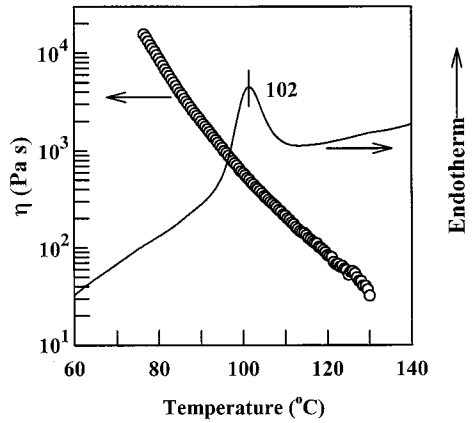

Figure 5. Variations of steady-state shear viscosity with temperature for PI-14-5CN (SCLCP) at $\dot{\gamma} = 0.1$ s^{-1}. The solid line is a DSC trace for PI-14-5CN at a heating rate of 20 °C/min.

It is seen from Figures 2b and 4a that the frequency dependencies of G'' and $|\eta^*|$ of PI-14-5CN, which is a nematic-forming SCLCP, look very similar to those often observed in flexible linear polymers. Referring to Figure 2b, it should be pointed out that at very low values of ω (say at $\omega < 0.1$ rad/s) in the nematic region (at temperatures below 105 °C) the values of G'' are about 1 order of magnitude greater than those of G'. Therefore, the calculated values of $|\eta^*|$ at $\omega < 0.1$ rad/s, given in Figure 4a, are determined predominantly by the values of G''. This now explains why the $|\eta^*|$ at low values of ω, given in Figure 4a, exhibits a Newtonian behavior, which follows from Figure 2b. On the other hand, from Figure 2a we observe that the frequency dependence of G' for PI-14-5CN in the nematic state is quite different from that in the isotropic state. Therefore, we conclude that the dynamic linear viscoelastic behavior of PI-14-5CN, which is an SCLCP, is *not* similar to that of flexible linear polymers.

Effect of Temperature on Steady-State Shear Viscosity. We investigated the temperature dependence of steady-state shear viscosity (η) for PI-14-5CN and PSHQ9, the results of which are given in Figures 5 and 6. In obtaining the results given in Figures 5 and 6, a shear rate of 0.1 s^{-1} was applied to a specimen, and the temperature was increased stepwise at a rate of 1 °C/min from the nematic state to the isotropic state. To facilitate our discussion, also given in Figures 5 and 6 are the DSC traces of the respective polymers. In Figures 5 and 6 we observe a striking difference in the temperature dependence of η between the two polymers. Specifically, Figure 5 shows that the η of PI-14-CN, which is an SCLCP, decreases steadily with increasing

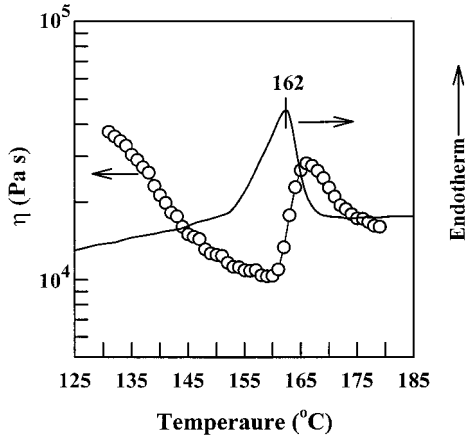

Figure 6. Variations of steady-state shear viscosity with temperature for PSHQ9 (MCLCP) at $\dot{\gamma} = 0.1$ s^{-1}. The solid line is a DSC trace for PSHQ9 at a heating rate of 20 °C/min.

temperature without exhibiting any abnormality as the polymer transforms from the nematic phase to the isotropic phase, very similar to the results reported previously by Colby et al.,[52] who also employed nematic SCLCPs.

On the other hand, in Figure 6 we observe a totally different temperature dependence of η for PSHQ9, which is an MCLCP. Namely, the η of PSHQ9 first decreases with increasing temperature as the specimen is heated from the nematic phase, then increases rapidly, going through a maximum, as the temperature approaches the T_{NI}, and then decreases again with increasing temperature further in the isotropic region. Earlier, similar observations were reported by other research groups[46,68,69] who also employed MCLCPs. According to Kim and Han,[46] (i) the decreasing trend of η in the nematic region of MCLCP is attributable, besides the usual Arrhenius effect, *in part* to an increase of the orientation of the nematic phase, (ii) the increasing trend of η before the temperature reaches T_{NI} is attributable to the formation of the biphasic region, giving rise to the higher weighted average of the η of the entire system as the amount of isotropic phase is increased in the biphasic region, and (iii) the decreasing trend of η with increasing temperature in the isotropic region is attributable to the usual Arrhenius effect. Referring to Figure 6, it should be mentioned that the gradual increase of η spanning over about 5 °C, instead of a very sharp increase, is believed to be due to the polydispersity of PSHQ9 (polydispersity index of about 2), because the low molecular portion of PSHQ9 might already have transformed into the isotropic state, forming a biphasic, before reaching T_{NI}.

A comparison of Figure 5 with Figure 6 indicates that under a very mild shear flow ($\dot{\gamma} = 0.1$ s^{-1}) the orientation of the side-chain 5CN-COOH mesogens that are grafted onto the PI-14-OH backbones has affected little the temperature dependence of η of PI-14-5CN in the nematic state, whereas the orientation of the nematic phase in PSHQ9, even under such a mild shear flow, has a profound influence on its temperature dependence of η in the nematic phase. Perhaps the difference in the temperature dependence of η between PI-14-5CN and PSHQ9 observed above may be characteristic of the differences in rheological responses between SCLCPs and MCLCPs in general.

Steady Shear-Flow Properties. Figure 7 gives log η vs log $\dot{\gamma}$ plots and log N_1 vs log $\dot{\gamma}$ plots for PI-14-5CN,

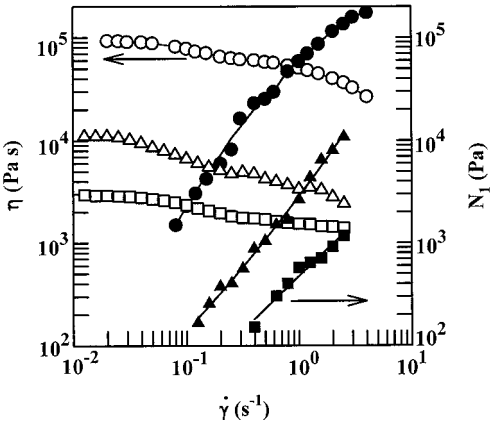

Figure 7. Plots of log η vs log $\dot{\gamma}$ (open symbols) and log N_1 vs log $\dot{\gamma}$ (filled symbols) for PI-14-5CN (SCLCP) at different temperatures in the nematic region: (○, ●) 70 °C; (△, ▲) 80 °C; (□, ■) 90 °C.

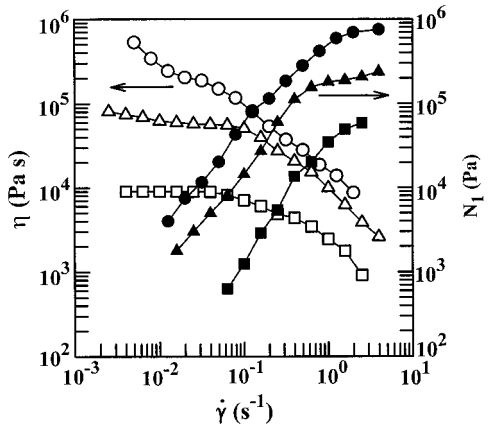

Figure 8. Plots of log η vs log $\dot{\gamma}$ (open symbols) and log N_1 vs log $\dot{\gamma}$ (filled symbols) for PSHQ9 (MCLCP) at different temperatures in the nematic region: (○, ●) 130 °C; (△, ▲) 140 °C; (□, ■) 150 °C.

which is an SCLCP, at 70, 80, and 90 °C in the nematic region for $\dot{\gamma}$ ranging from 0.01 to 3 s^{-1}, where N_1 is the steady-state first normal stress difference. It is seen in Figure 7 that the η of PI-14-5CN exhibits a Newtonian behavior at low $\dot{\gamma}$ and then shear-thinning behavior, usually observed for flexible linear polymers, and that values of N_1 for PI-14-5CN are *positive* over the entire range of $\dot{\gamma}$ tested at three different temperatures in the nematic region.

Figure 8 gives log η vs log $\dot{\gamma}$ plots and log N_1 vs log $\dot{\gamma}$ plots for PSHQ9, which is an MCLCP, at 130, 140, and 150 °C in the nematic region for $\dot{\gamma}$ ranging from 0.003 to 5 s^{-1}. From Figure 8 we observe that PSHQ9 also exhibits only *positive* values of N_1 over the entire range of $\dot{\gamma}$ tested and at three temperatures tested in the nematic region.

It is seen in Figure 8 that at 130 °C the η of PSHQ9 exhibits a shear-thinning behavior at very low values of $\dot{\gamma}$ (say $\dot{\gamma} < 0.01$ s^{-1}), a Newtonian behavior at intermediate values of $\dot{\gamma}$ (say 0.02 s$^{-1} < \dot{\gamma} < 0.05$ s^{-1}), and then, again, a strong shear-thinning behavior at higher values of $\dot{\gamma}$ (say $\dot{\gamma} > 0.1$ s^{-1}). In other words, the log η vs log $\dot{\gamma}$ plot for the MCLCP, PSHQ9, at 130 °C exhibits all three regions: regions I, II, and III following the notation of Onogi and Asada.[70] However, as the temperature is increased from 130 to 140 °C, region I in the log η vs log $\dot{\gamma}$ plot for PSHQ9 becomes very weak, and as the temperature is increased further to 150 °C

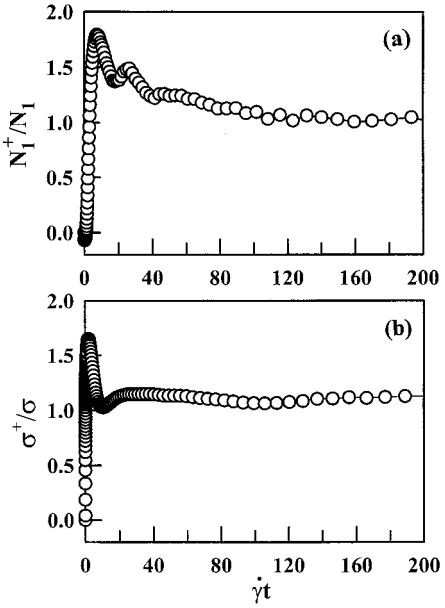

Figure 9. Time evolution of (a) $N_1^+(\dot{\gamma},t)/N_1$ and (b) $\sigma^+(\dot{\gamma},t)/\sigma$ for PI-14-5CN (SCLCP) at 70 °C upon start-up of shear flow at $\dot{\gamma} = 1.0\ s^{-1}$.

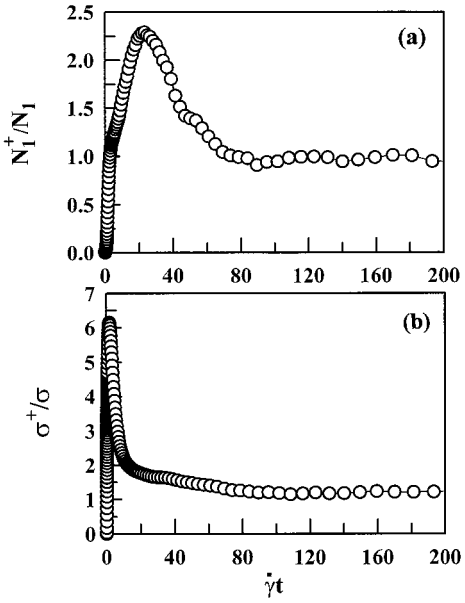

Figure 10. Time evolution of (a) $N_1^+(\dot{\gamma},t)/N_1$ and (b) $\sigma^+(\dot{\gamma},t)/\sigma$ for PSHQ9 (MCLCP) at 140 °C upon start-up of shear flow at $\dot{\gamma} = 1.0\ s^{-1}$.

region I disappears. The above observation supports the view that region I in the log η vs log $\dot{\gamma}$ plot for an LCP is associated with the existence of a domain structure.[71] The readers are reminded that the T_{NI} of PSHQ9 is ca. 160 °C (see Figure 6). Since PSHQ9 is a polydisperse polymer, the low molecular portion of PSHQ9 might begin to transform into the isotropic state, forming a biphasic, before reaching T_{NI}. Thus, the nematicity of PSHQ9 becomes progressively weaker as the temperature approaches its T_{NI}. Under such circumstances region I in the log η vs log $\dot{\gamma}$ plot for PSHQ9 may not be observable. This observation leads us to speculate tentatively that perhaps the nematicity in PI-14-5CN, which is an SCLCP, might not be sufficiently strong to exhibit region I in log η vs log $\dot{\gamma}$ plots, given in Figure 7. We thus conclude that the shear rate dependence of η is different between PI-14-5CN (SCLCP) and PSHQ9 (MCLCP).

A close look at Figures 7 and 8 reveals that at $\dot{\gamma} = 1.0\ s^{-1}$ the first normal stress difference and shear stress of PI-14-5CN at 70 and 80 °C are of the same magnitude, while the first normal stress difference of PSHQ9 at 130 and 140 °C is about an order of magnitude greater than the shear stress.

This observation suggests that, at an equal temperature below T_{NI}, the melt elasticity of PSHQ9, which is an MCLCP, is much greater than that of PI-14-5CN, which is an SCLCP.

Transient Shear Flow. Figure 9 describes normalized first normal stress difference $N_1^+(\dot{\gamma},t)/N_1$ and normalized shear stress $\sigma^+(\dot{\gamma},t)/\sigma$ with strain ($\dot{\gamma}t$) for PI-14-5CN (SCLCP) at 70 °C in the nematic region during transient shear flow at $\dot{\gamma} = 1.0\ s^{-1}$, where $N_1^+(\dot{\gamma},t)$ is the first normal stress difference growth and $\sigma^+(\dot{\gamma},t)$ is the shear stress growth upon start-up of shear flow.

It is seen in Figure 9 that both $N_1^+(\dot{\gamma},t)/N_1$ and $\sigma^+(\dot{\gamma},t)/\sigma$ go through a large overshoot and then decay to steady state. A similar observation can be made from Figure 10 for PSHQ9 (MCLCP).

The following observations are worth noting in Figures 9 and 10. Upon start-up of shear flow the overshoot peak in $N_1^+(\dot{\gamma},t)/N_1$ occurs much sooner in PI-14-5CN than in PSHQ9, while the overshoot peak in $\sigma^+(\dot{\gamma},t)/\sigma$ occurs very quickly in both PI-14-5CN and PSHQ9. The overshoot peak value of $N_1^+(\dot{\gamma},t)/N_1$ of PSHQ9 is slightly larger than that of PI-14-5CN, while the overshoot peak value of $\sigma^+(\dot{\gamma},t)/\sigma$ of PSHQ9 is about 3−4 times greater than that of PI-14-5CN. The overshoot peak values of $\sigma^+(\dot{\gamma},t)/\sigma$ and $N_1^+(\dot{\gamma},t)/N_1$ for PI-14-5CN are approximately the same, while the overshoot value of $\sigma^+(\dot{\gamma},t)/\sigma$ for PSHQ9 is about 3 times greater than that of $N_1^+(\dot{\gamma},t)/N_1$. We thus conclude that transient responses in first normal stress difference and shear stress for the SCLCP, PI-14-5CN, are different from those for the MCLCP, PSHQ9.

Intermittent Shear Flow. Figure 11 describes $N_1^+(\dot{\gamma},t)/N_1$ as a function of $\dot{\gamma}t$, and Figure 12 describes $\sigma^+(\dot{\gamma},t)/\sigma$ as a function of $\dot{\gamma}t$ for PI-14-5CN (SCLCP) at 70 °C in the nematic region (i) during transient shear flow for 1 h followed by a rest for 1 h upon cessation of shear flow and (ii) during intermittent shear flow for 1 h at three different shear rates: (a) at $\dot{\gamma} = 1.0\ s^{-1}$, (b) at $\dot{\gamma} = 0.5\ s^{-1}$, and (c) at $\dot{\gamma} = 0.1\ s^{-1}$. What is of great interest in Figures 11 and 12 is that not only is the shape of the responses of $N_1^+(\dot{\gamma},t)/N_1$ and $\sigma^+(\dot{\gamma},t)/\sigma$, respectively, during the intermittent shear flow very close to that during the transient flow, but also the size of the overshoot peak during the intermittent shear flow is as large as that upon start-up of shear flow! This observation suggests to us that, after a rest for 1 h upon cessation of shear flow, PI-14-5CN behaves as if it were a fresh specimen; i.e., the previous shear history of PI-14-5CN has disappeared completely after a rest for 1 h.

We conducted, also, transient/intermittent shear flow experiments for PI-14-5CN at $\dot{\gamma} = 1.0\ s^{-1}$ and 110 °C, which is slightly higher than its T_{NI} (102 °C). We have found, although the results are not presented here, that there is negligible overshoot in both $N_1^+(\dot{\gamma},t)$ and $\sigma^+(\dot{\gamma},t)$ in the isotropic phase, whereas there are very large overshoots in both $N_1^+(\dot{\gamma},t)$ and $\sigma^+(\dot{\gamma},t)$ in the nematic phase, and that the peak values of both $N_1^+(\dot{\gamma},t)$ and $\sigma^+(\dot{\gamma},t)$ in the nematic phase are 2 orders of magnitude greater than those in the isotropic phase. Further, we

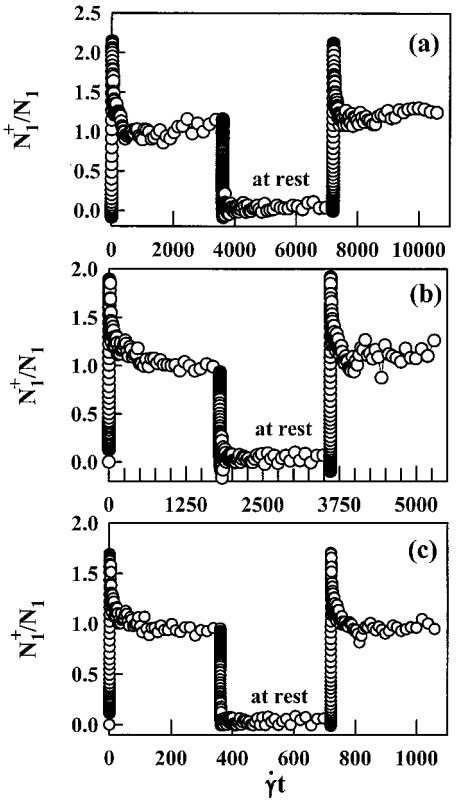

Figure 11. Variations of $N_1^+(\dot{\gamma},t)/N_1$ with $\dot{\gamma}t$ for PI-14-5CN (SCLCP) at 70 °C: (i) during transient shear flow (a) at $\dot{\gamma} = 1.0\ s^{-1}$, (b) at $\dot{\gamma} = 0.5\ s^{-1}$, and (c) at $\dot{\gamma} = 0.1\ s^{-1}$, (ii) during rest, and (iii) during intermittent shear flow (a) at $\dot{\gamma} = 1.0\ s^{-1}$, (b) at $\dot{\gamma} = 0.5\ s^{-1}$, and (c) at $\dot{\gamma} = 0.1\ s^{-1}$.

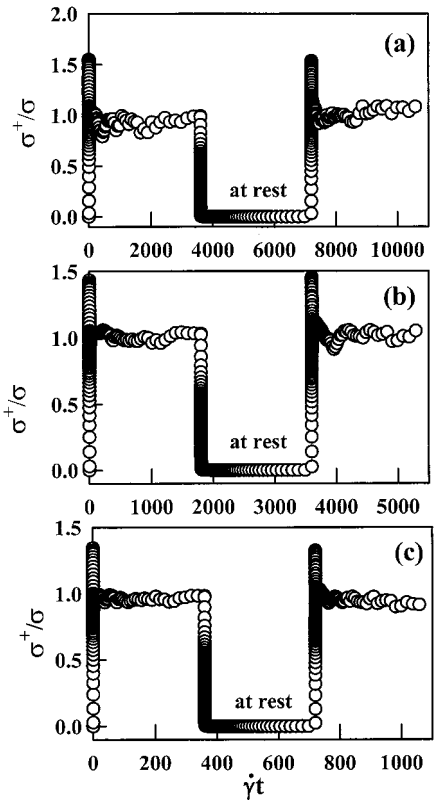

Figure 12. Variations of $\sigma^+(\dot{\gamma},t)/\sigma$ with $\dot{\gamma}t$ for PI-14-5CN (SCLCP) at 70 °C: (i) during transient shear flow (a) at $\dot{\gamma} = 1.0\ s^{-1}$, (b) at $\dot{\gamma} = 0.5\ s^{-1}$, and (c) at $\dot{\gamma} = 0.1\ s^{-1}$, (ii) during rest, and (iii) during intermittent shear flow (a) at $\dot{\gamma} = 1.0\ s^{-1}$, (b) at $\dot{\gamma} = 0.5\ s^{-1}$, and (c) at $\dot{\gamma} = 0.1\ s^{-1}$.

conducted transient/intermittent shear flow experiments for a very high molecular weight polyisoprene (PI), PI-270 having $M_n = 270\,000$ g/mol, at 200 °C and at $\dot{\gamma} = 1.0\ s^{-1}$. Here we chose homopolymer PI, because our SCLCP, PI-14-5CN, is based on the PI backbone. We have found, although the results are not presented here, that there is virtually *no* overshoot in $N_1^+(\dot{\gamma},t)$ and $\sigma^+(\dot{\gamma},t)$ for PI-270. Therefore, we conclude that the nonlinear transient rheology of PI-14-5CN presented in Figures 11 and 12 is attributable *solely* to the liquid crystallinity of the SCLCP, PI-14-5CN, and has no resemblance to the nonlinear transient rheology of the flexible homopolymer.

Figure 13 describes (a) variations of $N_1^+(\dot{\gamma},t)/N_1$ with $\dot{\gamma}t$ and (b) variations of $\sigma^+(\dot{\gamma},t)/\sigma$ with $\dot{\gamma}t$ for PSHQ9 (MCLCP) at 150 °C in the nematic region (i) during transient shear flow for 1 h followed by a rest for 1 h upon cessation of shear flow and (ii) during intermittent shear flow for 1 h at $\dot{\gamma} = 1.0\ s^{-1}$. It can be seen in Figure 13 that the value of the overshoot peak in both $N_1^+(\dot{\gamma},t)/N_1$ and $\sigma^+(\dot{\gamma},t)/\sigma$ during the intermittent shear flow is much smaller than that upon start-up of shear flow. The above observation is quite different from that made above in reference to Figures 11 and 12 for PI-14-5CN. A comparison of Figure 13 with Figures 11 and 12 indicates that deformation history has a profound influence on the subsequent shear flow of an MCLCP.

The difference in first normal stress difference and shear stress responses between PI-14-5CN and PSHQ9, shown above during intermittent shear flow, may be explained with the following observations. Since the 5CN-COOH mesogens are grafted onto the coillike PI forming a polymer backbone through five methylene

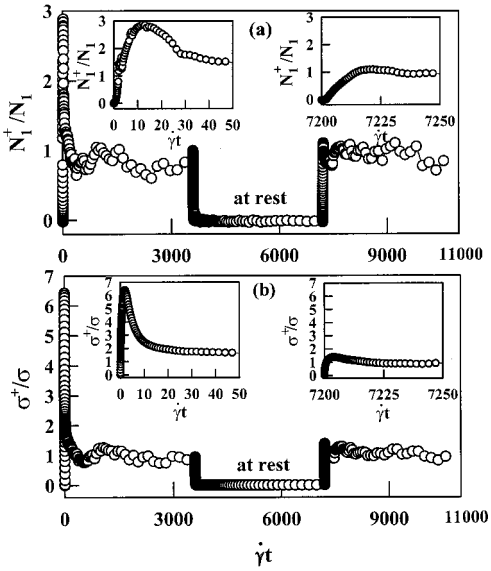

Figure 13. (a) Variations of $N_1^+(\dot{\gamma},t)/N_1$ with $\dot{\gamma}t$ and (b) variations of $\sigma^+(\dot{\gamma},t)/\sigma$ with $\dot{\gamma}t$ for PSHQ9 (MCLCP) at 150 °C: (i) during transient shear flow at and at $\dot{\gamma} = 1.0\ s^{-1}$, (ii) during rest, and (iii) during intermittent shear flow at $\dot{\gamma} = 1.0\ s^{-1}$.

groups as flexible spacer, the motions of the polymer backbone and the 5CN-COOH mesogens in PI-14-5CN may be regarded as being partially decoupled, making the 5CN-COOH mesogens mobile during shear flow. Further, each mesogen grafted onto the backbone of PI-14-5CN may move or orient, upon start-up of shear flow, little dependent upon other mesogens. On the other hand, the mesogens (phenyl groups) in PSHQ9 are directly linked to the polymer backbone, making the

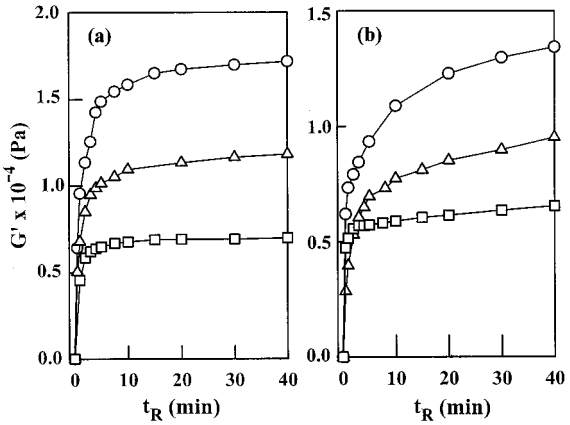

Figure 14. Time evolution of dynamic storage modulus G' upon cessation of steady-state shear flow at $\dot{\gamma} = 1.0\ s^{-1}$, which was monitored at an angular frequency of 1.0 rad/s for (a) PI-14-5CN (SCLCP) at different temperatures (○, 70 °C; △, 80 °C; □, 90 °C) and (b) PSHQ9 (MCLCP) at different temperatures (○, 130 °C; △, 140 °C; □, 150 °C).

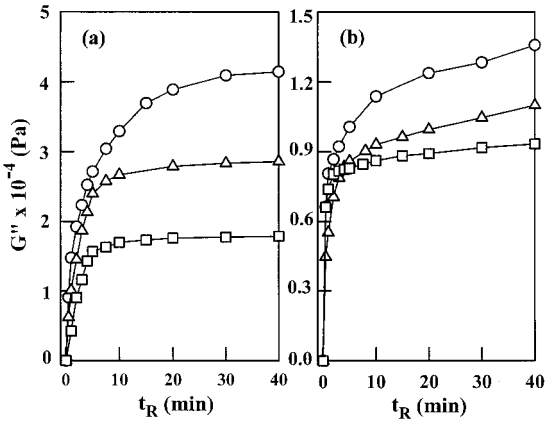

Figure 15. Time evolution of dynamic loss modulus G'' upon cessation of steady shear flow at $\dot{\gamma} = 1.0\ s^{-1}$, which was monitored at an angular frequency of 1.0 rad/s for (a) PI-14-5CN (SCLCP) at different temperatures (○, 70 °C; △, 80 °C; □, 90 °C) and (b) PSHQ9 (MCLCP) at different temperatures (○, 130 °C; △, 140 °C; □, 150 °C).

motions of the mesogens and backbone of PSHQ9 strongly coupled during shear flow. Thus, each mesogen in PSHQ9 cannot act as if it were independent from other mesogens. All the mesogens in PSHQ9 must act, upon start-up of shear flow, collectively or cooperatively.

It is then not difficult to speculate that the rheological response of the entire polymer chain of PSHQ9, which is an MCLCP, would be very sluggish, as compared to that of PI-14-5CN, which is an SCLCP. It seems then very reasonable to speculate that upon cessation of shear flow the stresses of the 5CN-COOH that are grafted as side chains through five methylene groups as flexible spacer onto the PI backbone in PI-14-5CN would relax much faster than the stresses of the mesogens (phenyl groups) that are linked directly to the polymer backbone of PSHQ9. In the same token, the time required for PI-14-5CN to return, upon cessation of shear flow, to the state of a randomly distributed equilibrium polydomain would be much shorter than that for PSHQ9. These speculations may now explain why the peak values of $N_1^+(\dot{\gamma},t)/N_1$ and $\sigma^+(\dot{\gamma},t)/\sigma$ for PI-14-5CN (SCLCP) during the intermittent shear flow after a rest for 1 h are almost the same as those observed during the transient shear flow, while the peak values of $N_1^+(\dot{\gamma},t)/N_1$ and $\sigma^+(\dot{\gamma},t)/\sigma$ for PSHQ9 (MCLCP) during the intermittent shear flow, after a rest for 1 h upon cessation of shear flow, are much smaller than those observed during the transient shear flow.

Time Evolution of Dynamic Moduli after Cessation of Shear Flow. In the present study we monitored time evolution of dynamic storage and loss moduli (G' and G'') upon cessation of shear flow by applying very small-amplitude oscillatory deformation to the specimen. Figure 14a gives time evolution of G' upon cessation of shear flow of a PI-14-5CN (SCLCP) specimen, which had been sheared at $\dot{\gamma} = 1.0\ s^{-1}$ for 1 h at 70, 80, or 90 °C. It is seen in Figure 14a that G' initially increases very rapidly and then increases slowly to reach a constant value about 10 min after cessation of shear flow when a specimen had been sheared at 90 °C, while it took about 40 min for the G' to reach a constant value when a specimen had been sheared at 70 °C, which is about 30 °C below the T_{NI} of PI-14-5CN. An increase of G' upon cessation of shear flow may be viewed as signifying a recovery of the deformed domain structure after the flow is stopped.[72] From this point of view we can understand why it takes a longer time for the G' to reach a constant value as the test temperature is farther away from the T_{NI} of PI-14-5CN. Figure 14b gives time evolution of G', upon cessation of shear flow, of a PSHQ9 (MCLCP) specimen, which had been sheared at $\dot{\gamma} = 1.0\ s^{-1}$ for 1 h at 130, 140, or 150 °C. It is seen in Figure 14b that G' initially increases very rapidly and then increases slowly. In contrast to the observation made above in reference to Figure 14a for PI-14-5CN, the G' of PSHQ9 does *not* attain a constant value even 40 min after cessation of shear flow when a specimen had been sheared at 130 °C, which is about 30 °C below the T_{NI} of PSHQ9. Comparison of parts a and b of Figure 14 clearly shows that, at the same applied shear rate and also at an equal temperature from T_{NI}, the recovery of the deformed domain structure is much slower in the MCLCP than in the SCLCP. A similar trend is observed in Figure 15, where time evolution of G'' after cessation of shear flow is given for PI-14-5CN and PSHQ9. The differences in the time evolution of G' and G'', upon cessation of shear flow, between PI-14-5CN (SCLCP) and PSHQ9 (MCLCP) can be explained using the same argument that was presented above to explain the differences in the intermittent shear flow between the two polymers.

It should be mentioned at this juncture that, using solutions of PBLG in *m*-cresol, Moldenaers and Mewis[39,73,74] reported that G' and G'' *decreased* with time after cessation of shear flow. Such an experimental observation was predicted by Larson and Mead.[75] On the other hand, using aqueous solutions of hydroxypropylcellulose, Grizzuti et al.[35] reported that G' and G'' *increased* with time after cessation of shear flow, showing the same trend as that given in Figures 14 and 15 above and also in a paper by Kim and Han,[72] who employed an MCLCP. At present we do not have theory that can explain the two opposite experimental observations.

Stress Relaxation upon Cessation of Shear Flow. In this study we investigated the relaxation of stresses upon cessation of shear flow by recording both shear stress decay $\sigma^-(\dot{\gamma},t)$ and first normal stress difference decay $N_1^-(\dot{\gamma},t)$. Figures 16 describes the decay of normalized shear stress $\sigma^-(\dot{\gamma},t)/\sigma_0$ with time t_R after cessation of shear flow for (a) PI-14-5CN that had been sheared at 70 °C and at $\dot{\gamma} = 0.1$, 0.5, or 1.0 s^{-1} and (b)

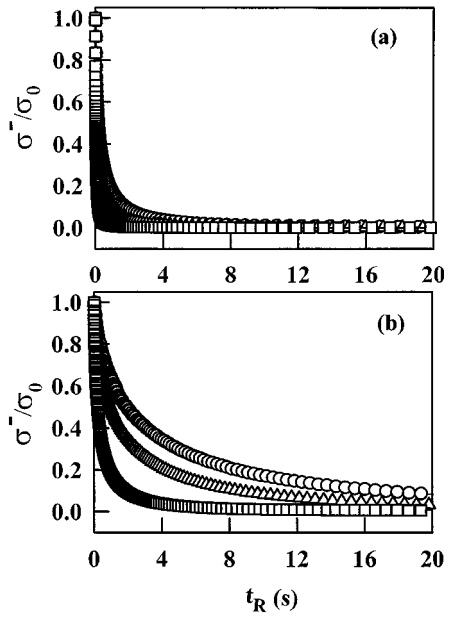

Figure 16. Relaxation of normalized shear stress, $\sigma^-(\dot{\gamma},t)/\sigma_0$, upon cessation of steady shear flow at different shear rates: (○) $\dot{\gamma} = 1.0$ s^{-1}; (△) $\dot{\gamma} = 0.5$ s^{-1}; (□) $\dot{\gamma} = 0.1$ s^{-1} for (a) PI-14-5CN (SCLCP) at 70 °C and (b) PSHQ9 (MCLCP) at 130 °C, where σ_0 is the steady-state shear stress just prior to flow cessation.

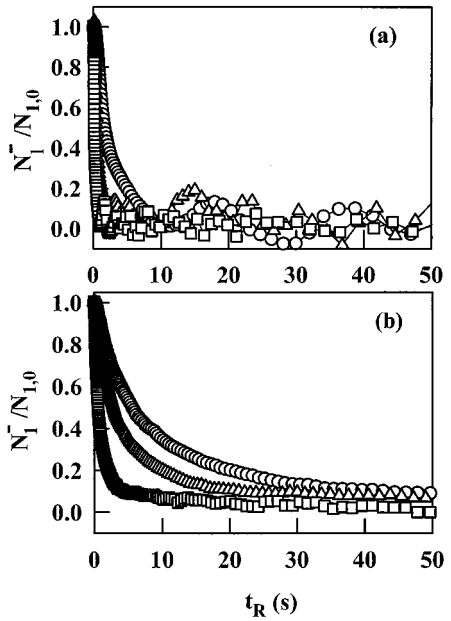

Figure 17. Relaxation of normalized first normal stress difference, $N_1^-(\dot{\gamma},t)/N_{1,0}$, upon cessation of steady shear flow at different shear rates: (○) $\dot{\gamma} = 1.0$ s^{-1}; (△) $\dot{\gamma} = 0.5$ s^{-1}; (□) $\dot{\gamma} = 0.1$ s^{-1} for (a) PI-14-5CN (SCLCP) at 70 °C and (b) PSHQ9 (MCLCP) at 130 °C, where $N_{1,0}$ is the steady-state first normal stress difference just prior to flow cessation.

PSHQ9 that had been sheared at 130 °C and at $\dot{\gamma} =$ 0.1, 0.5, or 1.0 s^{-1}, where σ_0 is the shear stress just prior to cessation of shear flow. In Figure 16 we observe that the relaxation rate of shear stress is slower as the applied shear rate during shear flow is increased. This is understandable, because the higher the applied shear rate, the greater the amount of shear stresses accumulated in the specimen and thus the longer it will take for the shear stress to completely relax after cessation of shear flow. It is clearly seen in Figure 16 that the rate of shear stress relaxation is much slower in PSHQ9 (MCLCP) than in PI-14-5CN (SCLCP). Again, this difference describes how slow is the recovery, after cessation of shear flow, of the domain texture in MCLCP, as compared to that in SCLCP. As discussed above in reference to Figures 11−13, the 5CN-COOH grafted on the coillike backbone of PI, forming PI-14-5CN (SCLCP), might be very mobile and thus would relax rather quickly upon cessation of shear flow, as compared to the mesogens (phenyl groups) that are linked directly to the polymer backbone of PSHQ9 (MCLCP).

Figure 17 describes the decay of normalized first normalized stress difference $N_1^-(\dot{\gamma},t)/N_1$ with t_R after cessation of shear flow for (a) PI-14-5CN (SCLCP) that had been sheared at 70 °C and at $\dot{\gamma} =$ 0.1, 0.5, or 1.0 s^{-1} and (b) PSHQ9 (MCLCP) that had been sheared at 130 °C and at $\dot{\gamma} = 0.1$, 0.5, or 1.0 s^{-1}, where $N_{1,0}$ is the first normal stress difference just prior to cessation of shear flow. In Figure 17 we observe that the relaxation rate of first normal stress difference is slower as the applied shear rate during shear flow is increased, very similar to that observed for the shear stress relaxation in Figure 16, and that the relaxation of first normal stress difference in PSHQ9 (MCLCP) is much slower than that in PI-14-5CN (SCLCP). However, a very unusual relaxation behavior of PI-14-5CN can be seen in Figure 17 in that the first normal stress difference, upon cessation of shear flow, first decreases rapidly and then fluctuates near the baseline (zero value). We have observed this behavior with repeated experiments using fresh PI-14-5CN specimens, while we did not observe any such fluctuations of first normal stress difference when using PSHQ9 specimen. We tentatively attribute the sustained oscillations near the baseline, after cessation of shear flow, of first normal stress difference of PI-14-5CN to the unsettling motions of the 5CN-COOH mesogens that are grafted onto the coillike PI forming the polymer backbone through five methylene groups as flexible spacer. That is, the motions of the polymer backbone and the 5CN-COOH mesogens in the SCLCP, PI-14-5CN, may be regarded as being partially decoupled, making the side-chain 5CN-COOH mesogens move somewhat freely after cessation of shear flow. At present this observation is just a speculation, and a more systematic investigation of this subject is worth pursuing in the future.

4. Concluding Remarks

It is well accepted today that transient shear flow and stress relaxation are much more sensitive to the differences in chemical structures of polymeric liquids than steady or oscillatory shear flows. This is particularly so when dealing with structured polymeric liquids, such as thermotropic LCPs investigated in the present study. In this paper we have compared the linear dynamic viscoelasticity, steady shear-flow properties, rheological responses to transient and intermittent shear flows, and the relaxation of shear stress and first normal stress difference upon cessation of shear flow of a newly synthesized SCLCP, PI-14-5CN, vis-à-vis with the rheological behavior of an MCLCP, PSHQ9.

The comparison has revealed several interesting observations presented above, which have not been reported in the literature. From the results obtained in the present study we conclude that the stress relaxation and the recovery of domain structure, upon cessation of shear flow, are much faster in the SCLCP than in

the MCLCP. We attribute the observed differences in the rheological behavior between the SCLCP and MCLCP to the differences in the mobility of mesogens present in the respective thermotropic LCPs. Specifically, we have pointed out that the mesogens (phenyl groups) that are linked directly to the polymer backbone of PSHQ9 make the mesogens and the backbone strongly coupled during shear flow, which then would result in slower stress relaxation and slower recovery of domain structure upon cessation of shear flow, as compared to the situation where the 5CN-COOH mesogens are grafted as side chains, through methylene groups as flexible spacer, onto the coillike polymer backbone forming PI-14-5CN.

Before closing, we wish to point out the uniqueness of PI-14-5CN synthesized in this study for rheological investigations. PI-14-5CN is a nearly monodisperse SCLCP that has advantages over polydisperse SCLCPs. This was made possible by the synthetic route employed in this study; namely, a nearly monodisperse PI was first synthesized via anionic polymerization and then hydroxylated to still yield a nearly monodisperse PI-OH. Grafting of a liquid crystalline monomer (5CN-COOH in the present study) onto the hydroxyl groups of PI-OH yielded a nearly monodisperse SCLCP. It should be mentioned that most of the SCLCPs and MCLCPs reported in the literature have been prepared by condensation polymerization, invariably yielding polydisperse polymers. Using the synthetic route described in this paper, the molecular weight of SCLCPs can be controlled very accurately, which would not be easy when using condensation polymerization. Further, by adopting the synthetic route described in this paper, one can easily vary the extent of liquid crystallinity in an SCLCP by controlling the extent of hydroxylation of PI-OH. Specifically, one can hydroxylate only 30, 50, 70, or 80% of the 1,2- and 3,4-addition in an anionically synthesized PI in THF as solvent and then graft liquid crystalline monomers onto the hydroxylated PI-OH. In so doing, one can control the viscosity and first normal stress difference of the resulting SCLCP at any desired levels, which would not be easy when using condensation polymerization. Further, one can easily graft any type of liquid crystalline monomer (nematic, smectic, or cholesteric mesogens) as long as it has the proper functional groups, onto a PI-OH, so that nematic, smectic, or cholesteric SCLCP can easily be obtained. Again, such flexibility cannot easily be realized when using condensation polymerization. Thus, the synthetic route described in this paper would be very useful to prepare model SCLCPs for rheological investigation.

Acknowledgment. We acknowledge that this study was supported in part by the National Science Foundation under Grant CTS-9981972, and reviewers' constructive comments helped us to improve the original manuscript.

References and Notes

(1) Kiss, G.; Porter, R. S. *Mol. Cryst. Liq. Cryst.* **1980**, *60*, 267.
(2) Doppert, H. L.; Picken, S. J. *Mol. Cryst. Liq. Cryst.* **1987**, *153*, 109.
(3) Moldenaers, P.; Fuller, G.; Mewis, J. *Macromolecules* **1989**, *22*, 960.
(4) Hongladarom, K.; Burghardt, W. R.; Baek, S. G.; Cementwala, S.; Magda, J. J. *Macromolecules* **1993**, *26*, 772.
(5) Hongladarom, K.; Burghardt, W. R. *Macromolecules* **1993**, *26*, 785.
(6) Hongladarom, K.; Secakusuma, V.; Burghardt, W. R. *J. Rheol.* **1994**, *38*, 1505.
(7) Hongladarom, K.; Ugaz, V. M.; Cinader, D. K.; Burghardt, W. R.; Quintana, J. P.; Hsiao, B. D.; Dadmun, M. D.; Hamilton, W. A.; Butler, P. D. *Macromolecules* **1996**, *29*, 5346.
(8) Hsiao, B. S.; Stein, R. S.; Deutscher, L.; Winter, H. H. *J. Polym. Sci., Polym. Phys. Ed.* **1990**, *28*, 1571.
(9) Mather, P.; Jeon, D. F.; Han, C. D.; Chang, S. *Macromolecules* **2000**, *33*, 7579.
(10) Kim, D.-O.; Han, C. D.; Mather, P. *Macromolecules* **2000**, *33*, 7922.
(11) Picken, S. J.; Aerts, J.; Visser, B.; Northolt, M. G. *Macromolecules* **1990**, *23*, 3849.
(12) Odell, J. A.; Ungar, G.; Feijoo, J. L. *J. Polym. Sci., Polym. Phys. Ed.* **1993**, *31*, 141.
(13) Gervat, L.; MacKley, M. R.; Nicholson, T. M.; Windle, A. J. *Philos. Trans. R. Soc. London A* **1995**, *350*, 1.
(14) Ugaz, V. M.; Burghardt, W. R. *Macromolecules* **1998**, *31*, 8474.
(15) Kernick, W. A.; Wagner, N. J. *Macromolecules* **1999**, *32*, 1159.
(16) Zhou, W.-J.; Kornfield, J. A.; Ugaz, V. M.; Burghardt, W. R.; Link, D. R.; Clark, N. A. *Macromolecules* **1999**, *32*, 5581.
(17) Alderman, N. J.; MacKley, M. R. *Faraday Discuss. Chem. Soc.* **1985**, *79*, 149.
(18) De'Nève, T.; Navard, P.; Kleman, M. *J. Rheol.* **1993**, *37*, 515.
(19) Gleeson, J. T.; Larson, R. G.; Mead, D. W.; Kiss, G.; Cladis, P. E. *Liq. Cryst.* **1992**, *11*, 341.
(20) Larson, R. G.; Mead, D. W. *Liq. Cryst.* **1992**, *12*, 751.
(21) Picken, S. J.; Aerts, J.; Doppet, H. L.; Ruevers, A. J.; Northolt, M. G. *Macromolecules* **1991**, *24*, 1366.
(22) Walker, L. M.; Kernick, W. A.; Wagner, N. J. *Macromolecules* **1997**, *30*, 508.
(23) Papkov, S. P.; Kulichikhin, B. G.; Kalmykovam, V. D.; Malkin, A. Ya. *J. Polym. Sci., Polym. Phys.* **1974**, *12*, 1753.
(24) Helminiak, T. E.; Berry, G. C. *J. Polym. Sci., Polym. Symp.* **1979**, *65*, 107.
(25) Wong, C. P.; Ohnuma, H.; Berry, G. C. *J. Polym. Sci., Polym. Symp.* **1979**, *65*, 173.
(26) Hermans, J. *J. Colloid Sci.* **1962**, *17*, 638.
(27) Kiss, G.; Porter, R. S. *J. Polym. Sci., Polym. Symp.* **1978**, *65*, 193.
(28) Asada, T.; Muramatsu, H.; Watanabe, R.; Onogi, S. *Macromolecules* **1980**, *13*, 867.
(29) Moldenaers, P.; Mewis, J. *J. Rheol.* **1986**, *30*, 567.
(30) Baek. S. G.; Magda, J.; Larson, R. G. *J. Rheol.* **1993**, *78*, 1201.
(31) Mewis, J.; Moldenaers, P. *Mol. Cryst. Liq. Cryst.* **1987**, *153*, 291.
(32) Walker, L. M.; Wagner, N. J.; Larson, R. G.; Mirau, P. A.; Moldenaers, P. *J. Rheol.* **1995**, *39*, 925.
(33) Walker, L. M.; Mortier, M.; Moldenaers, P. *J. Rheol.* **1996**, *40*, 967.
(34) Baek, S. G.; Magda, J. J.; Cementwala, S. *J. Rheol.* **1993**, *78*, 935.
(35) Grizzuti, N.; Cavella, S.; Cicarelli, P. *J. Rheol.* **1990**, *30*, 1293.
(36) Navard, P.; Haudin, J. M. *J. Polym. Sci., Polym. Phys.* **1986**, *24*, 189.
(37) Kiss, G.; Porter, R. S. *J. Polym. Sci., Polym. Phys. Ed.* **1980**, *18*, 361.
(38) Navard, P.; Haudin, J. M. *J. Polym. Sci., Polym. Phys. Ed.* **1986**, *24*, 189.
(39) Moldenaers, P.; Mewis, J. *J. Rheol.* **1986**, *30*, 567.
(40) Baek, S.-G.; Magda, J. J.; Larson, R. G. *J. Rheol.* **1993**, *37*, 1201.
(41) Baek, S.-G.; Magda, J. J.; Larson, R. G.; Hudson, S. D. *J. Rheol.* **1994**, *38*, 1473.
(42) Cocchini, F.; Nobile, M. R.; Acierno, D. *J. Rheol.* **1991**, *35*, 1171.
(43) Driscoll, P.; Masuda, T.; Fujiwara, K. *Macromolecules* **1991**, *24*, 1567.
(44) Kim, S. S.; Han, C. D. *J. Rheol.* **1993**, *37*, 847.
(45) Kim, S. S.; Han, C. D. *Macromolecules* **1993**, *26*, 6633.
(46) Kim, S. S.; Han, C. D. *J. Polym. Sci., Polym. Phys. Ed.* **1994**, *32*, 371.
(47) Chang, S.; Han, C. D. *Macromolecules* **1997**, *30*, 2021.
(48) Chang, S.; Han, C. D. *Macromolecules* **1997**, *30*, 1656.
(49) Kim, D.-O.; Han, C. D. *Macromolecules* **2000**, *33*, 3349.
(50) Zentel, R.; Wu, J. *Makromol. Chem.* **1986**, *187*, 1727.
(51) Fabre, P.; Veyssie, M. *Mol. Cryst. Liq. Cryst. Lett.* **1987**, *4*, 99.
(52) Colby, R. H.; Gillmor, J. R.; Galli, G.; Laus, M.; Ober, C. K.; Hall, E. *Liq. Cryst.* **1993**, *13*, 233.

(53) Kannan, R. M.; Kornfield, J. A. *Macromolecules* **1993**, *26*, 2050.
(54) Kannan, R. M.; Rubin, S. F.; Kornfield, J. A.; Boeffel, C. *J. Rheol.* **1994**, *38*, 1609.
(55) Rubin, S. F.; Kannan, R. M.; Kornfield, J. A.; Boeffel, C. *Macromolecules* **1995**, *28*, 3521.
(56) Grabowski, D. A.; Schmitdt, C. *Macromolecules* **1994**, *27*, 2632.
(57) Berghausen, J.; Fuchs, J.; Richtering, W. *Macromolecules* **1997**, *30*, 7574.
(58) Colby, R. H.; Ober, C. K.; Gilmor, J. R.; Connelly, R. W.; Duong, T.; Galli, G.; Laus, M. *Rheol. Acta* **1997**, *36*, 498.
(59) Quijada-Garrido, I.; Siebert, H.; Friedrich, C.; Schmidt, C. *Rheol. Acta* **1999**, *38*, 3495.
(60) Quijada-Garrido, I.; Siebert, H.; Friedrich, C.; Schmidt, C. *Macromolecules* **2000**, *33*, 3844.
(61) Wewerka, A.; Viertler, K.; Vlassopoulos, D.; Stelzer, F. *Rheol. Acta* **2001**, *40*, 416.
(62) Wewerka, A.; Floudas, G.; Pakula, T.; Stelzer, F. *Macromolecules* **2001**, *34*, 8129.
(63) Lee, K. M.; Han, C. D. *Macromolecules*, **2002**, *35*, 760.
(64) Lee, K. M.; Han, C. D. *Macromolecules*, **2002**, *35*, 3145.
(65) Chang, S.; Han, C. D. *Macromolecules* **1997**, *30*, 1670.
(66) Furukawa, A.; Lenz, R. W. *Macromol. Chem. Macromol. Symp.* **1986**, *2*, 3.
(67) Kim, S. S.; Han, C. D. *Polymer* **1994**, *35*, 93.
(68) Wunder, S. L.; Ramachandran, S.; Cochanour, C. R.; Weinberg, M. *Macromolecules* **1986**, *19*, 1696.
(69) Irwin, R. S.; Sweeny, W.; Gardner, K. H.; Gochanour, C. R.; Weinberg, M. *Macromolecules* **1989**, *22*, 1065.
(70) Onogi, S.; Asada, T. In *Rheology*; Astarita, G., Marrucci, G., Nicolias, L., Eds.; Plenum Press: New York, 1980; Vol. 1, p 127.
(71) Larson, R. G. *The Structure and Rheology of Complex Fluids;* Oxford University Press: Oxford, 1999.
(72) Kim, S. S.; Han, C. D. *J. Rheol.* **1994**, *38*, 13.
(73) Moldenaers, P.; Yanase, H.; Mewis, J. *J. Rheol.* **1991**, *35*, 1681.
(74) Moldenaers, P.; Mewis, J. *J. Rheol.* **1993**, *37*, 367.
(75) Larson, R. G.; Mead, D. W. *J. Rheol.* **1989**, *33*, 185.

MA012240K